AIDA

Advanced European Infrastructures for Detectors at Accelerators

Journal Publication

Radiation resistance of double-type double-sided 3D pixel sensors

Fernandez, M (CSIC) *et al*

21 December 2013

The research leading to these results has received funding from the European Commission under the FP7 Research Infrastructures project AIDA, grant agreement no. 262025.

This work is part of AIDA Work Package **9: Advanced infrastructures for detector R&D**.

The electronic version of this AIDA Publication is available via the AIDA web site <http://cern.ch/aida> or on the CERN Document Server at the following URL: <http://cds.cern.ch/search?p=AIDA-PUB-2013-036>

Nuclear Instruments and Methods in Physics Research A 732 (2013) 137–140

Contents lists available at ScienceDirect

Nuclear Instruments and Methods in Physics Research A

journal homepage: www.elsevier.com/locate/nima

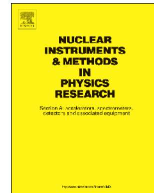

Radiation resistance of double-type double-sided 3D pixel sensors

M. Fernandez [a], R. Jaramillo [a], M. Lozano [b], F.J. Munoz [a,*], G. Pellegrini [b], D. Quirion [b], T. Rohe [c], I. Vila [a]

[a] Instituto de Física de Cantabria IFCA (CSIC-UC), Avd. de los Castros s/n, 39005 Santander, Spain
[b] Centro Nacional de Microelectrónica de Barcelona IMB-CNM (CSIC), Campus Univ. Autónoma de Barcelona, 08193 Bellaterra, Spain
[c] Paul Sherrer Institute PSI, 5232 Villigen, Switzerland

ARTICLE INFO

Available online 3 June 2013

Keywords:
Vertex detectors
Position sensitive detectors
Radiation-hard detectors
Solid state detectors

ABSTRACT

The proposed high-luminosity upgrade of the Large Hadron Collider is expected to increase the instantaneous luminosity at the experiments' interaction points by a factor of ten. The vertex detector will be the subsystem most affected by the luminosity increase, raising substantially their occupancy and radiation-induced damage. To preserve the vertex physics performance under these new conditions, current pixel technologies have to be improved. Hybrid pixel sensors with double-sided double-type vertical electrodes (3D sensors) are becoming a mature technology for the detector layers closest to the interaction point due to their intrinsic radiation hardness. In addition, the double-sided implementation of the 3D pixel technology provides some additional technical advantages with respect to the single-sided implementation. For this study, 3D pixel sensors manufactured at the Centro Nacional de Microelectrónica of Barcelona (IMB-CNM) have been bonded to the PSI46 readout chip currently used by the Compact Muon Solenoid vertex detector. Detector performance before and after irradiation up to fluences of 5×10^{15} n_{eq}/cm^2 is presented.

© 2013 Elsevier B.V. All rights reserved.

1. Introduction

The High Luminosity Large Hadron Collider (HL-LHC) is one of the possible Large Hadron Collider (LHC) upgrade options. After this upgrade the luminosity would increase considerably reaching a total integrated luminosity of 3000 fb^{-1} at the end of the running period. In this high luminosity scenario, the hadron fluences at the innermost layers of the experiments are expected to reach values up to 2×10^{16} n_{eq}/cm^2. Under these hostile conditions, silicon-based vertex detectors will suffer severely from radiation damage: increase of the leakage current, change in effective doping concentration of the bulk and reduction of charge collection efficiency due to the increase of radiation-induced defects.

By reducing the charge carriers collection distance, their probability for getting trapped in one of the radiation-induced defects decreases as well as the voltage needed to fully deplete the device. One way to reduce the collection distance is by shortening the distance between electrodes. In current planar technologies the electrode's distance is given by the sensor thickness, therefore thinner sensors will be needed reducing the collected charge as well.

One alternative technology is the so-called 3D sensors, these sensors have a vertical array of electrodes that penetrate into the detector bulk [1]. Electrons and holes, moving parallel to the sensor surface, are then collected at opposite biased cylindrical electrodes. Minimum drift time and depletion voltage are determined by the electrode spacing and the charge carriers generated by ionizing radiation can be collected within a time smaller than the trapping time of the radiation-induced defects [2].

Studies comparing standard microstrip detectors fabricated in p-type material and 3D strip detectors made in the same type of silicon material [3] have shown the superiority of 3D detectors for fluences up to 2×10^{15} n_{eq}/cm^2. This paper reports the results of the characterization of 3D double-sided and double-type pixel detectors before and after irradiation up to 5×10^{15} n_{eq}/cm^2.

2. Device description

The studied sensors were manufactured at the Centro Nacional de Microelectrónica of Barcelona (IMB-CNM). Out of the six wafers of the production batch, five were 285 μm thick and one 230 μm thick. In addition, the pixel devices in one of the thick wafers were manufactured with a polysilicon resistance grid to compare the electric characterization of the devices biased either through the resistors grid (resistor biasing) or the guard ring (punch-through biasing).

* Corresponding author.
E-mail addresses: fjmunoz@ifca.unican.es, fmunoz@cern.ch (F.J. Munoz).

0168-9002/$ - see front matter © 2013 Elsevier B.V. All rights reserved.
http://dx.doi.org/10.1016/j.nima.2013.05.121

In the wafer layout several devices were included: one multi-chip module, with a matrix of 8×2 single sensors; twenty single chip sensors, with different geometries; eight strip detectors, where all the n-type electrodes along a line are shorted by an aluminum track; and twelve pad detectors. The multi-chip module has the same layout as the current CMS planar pixel module.

A basic pixel cell in n-on-p technology consists of one n-type vertical electrode with a diameter of 10 μm, surrounded by a p-stop insulation ring of internal and external diameters 10 and 15 μm respectively. On the backside, 10 μm diameter p-type 3D electrodes, creating the ohmic contacts, are arranged surrounding the n+ electrode. The pixel layout matches the PSI46 chip layout [4], which is the readout ASIC used in the current CMS vertex detector. A picture of the pixel cell where the polysilicon resistor routing is visible and a scanning electron microscope picture after the bump reflow process are shown in Fig. 1.

The proposed [5] double-sided 3D detectors, shown in Fig. 2, are fabricated in a double-type configuration, with columns of one doping type etched from the front side of the device, and the other type etched from the back side. Neither set of columns pass through the full thickness of the silicon substrate. The double side structure is similar to a conventional 3D detector [6], but has a simpler fabrication process because the difficulty of doping the two different kinds of holes on the same side is avoided. The photolithographic steps needed to define the electrode contacts in the polysilicon layer are only necessary on the top surface. The polysilicon on the bottom surface does not need any patterning since it shorts all the holes together. This allows to apply the high voltage bias to the back surface of the detector by simple wire bonding. This avoids complicated rerouting in detectors for readout electronics which do not have any structure to apply the bias from the bonded side. The interconnection process between sensor and readout chip, which includes bump bonding and flip-chip, has been done at Paul Sherrer Institute (PSI) bonding laboratory.

3. Electrical characterization

Sensors from six wafers have been electrically characterized. Sensor nomenclature and characteristics are listed in Table 1.

Exhaustive measurements of *I–V* curves have been carried out in all pixel devices for each wafer. The results show an homogeneous behavior for all devices in the same wafer, and the leakage current values are below 100 nA in four wafers (70% of sensors), while two wafers show higher current values reaching in the worst cases more than 100 μA. Fig. 3 shows an example of *I–V* curves for four single-chips and one multi-chip sensor on wafer 6. Letter B indicates the sensor position in the wafer. Differences between devices in the same wafer are below 100 nA and as expected the multi-chip (sixteen single-chips) has higher leakage current.

One of the aims of the electrical characterization was to assess the advantages and drawbacks of integrating a polysilicon resistor grid in the pixel sensor design. This resistive biasing grid allows the full depletion of the sensor without the need of bonding it to the readout ASIC. This enables easier electrical testing and qualification of the sensor before it is bonded, one of the most expensive and time consuming part of the fabrication of a pixel module. We have measured the current–voltage (*I–V*) characteristic with two different biasing configurations: through the bias ring and by means of the guard ring (punch-through biasing). The results are presented in Fig. 4, for one single detector. No relevant differences are found, biasing the sensor through the

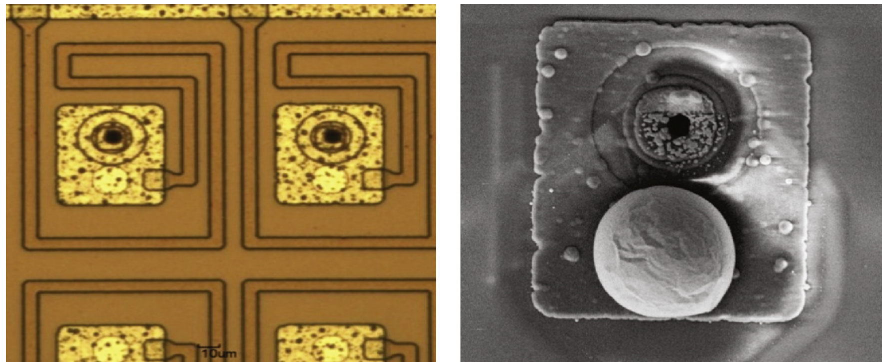

Fig. 1. Left: sensor pixel cells where the polysilicon resistor routing is visible. Right: SEM picture of one pixel cell, where the indium ball is shown as well as the n-doped column with the p-stop surrounding it. The ohmic holes (p+ doped) are on the backside and they are not visible from the front side.

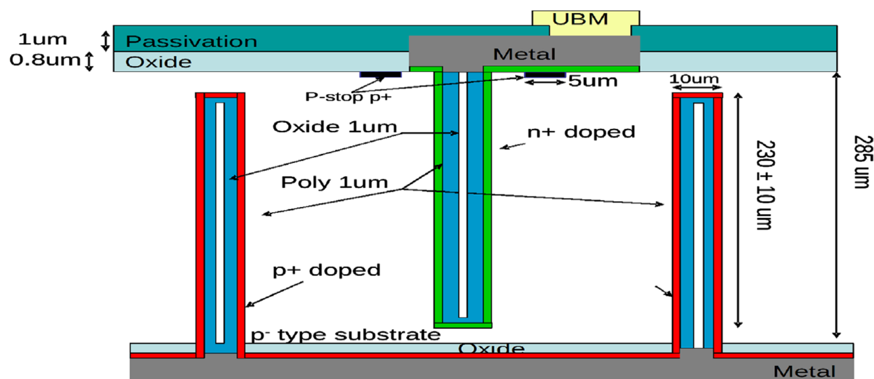

Fig. 2. Schematic of a 3D double sided detector.

Table 1
Description of the devices included in each wafer.

Device name	Qty	Description
MC	1	Multi-chip module (8 × 2 detectors)
SC 11, 12, 21, 22	20	Single chip detector with different geometries
3D strip	8	Strip detector
3D pads	12	Pad detector

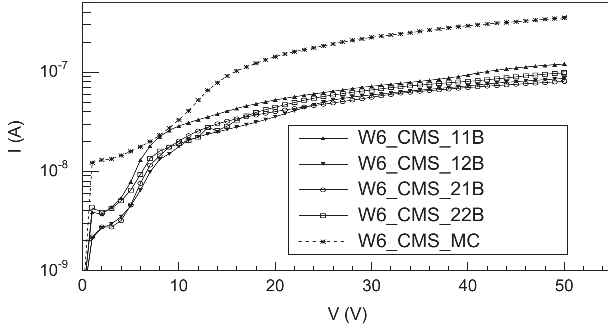

Fig. 3. Current voltage characteristics of the sensors in one wafer (wafer 6) 285 μm thick, four single chips and one multi-chip (8 × 2).

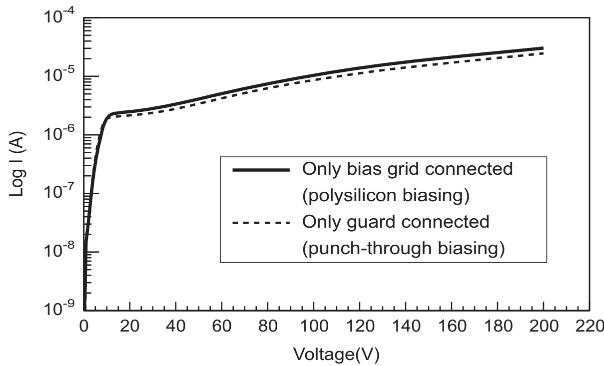

Fig. 4. Current voltage characteristics of one sensor with the polysilicon bias grid. Continuous line shows the measurement biasing through the polysilicon grid. Dashed line shows the measurement biasing by punch-through.

polysilicon resistor grid or by punch-through. Another important result shown in this figure is that no breakdown is observed before 200 V.

The capacitance–voltage (C–V) characteristic was determined using an LCR meter and an auxiliary circuit for decoupling the high voltage bias and the input signal to the LCR meter. The frequency of the AC signal to measure the C–V curves was fixed at 10 kHz and the amplitude at 100 mV. From these curves, the value of the full depletion voltage (V_{fd}) of the 3D pad sensors was extracted by the standard algorithm of finding the intersection point between the two straight lines fitting the ramp-up and plateau sections of the $1/C^2$ curve which is shown in Fig. 5. The depletion voltage extracted from the 3D pad detectors has been used to analytically determine the depletion voltage of the single-chip and multi-chip sensors using the expression for a true coaxial electrode given by Eq. (1) [7,8], where r_1 and r_2 are the electrode column outer radius and the distance between p+ and n+ doped columns respectively, N is the impurity density in the bulk, q is the electronic charge, and ϵ is the dielectric constant of silicon. Using these parameters and the measured 3D pad depletion voltage as inputs, the assessed full depletion voltage for the pixel detectors is 9 V. A working voltage of 20 V has been

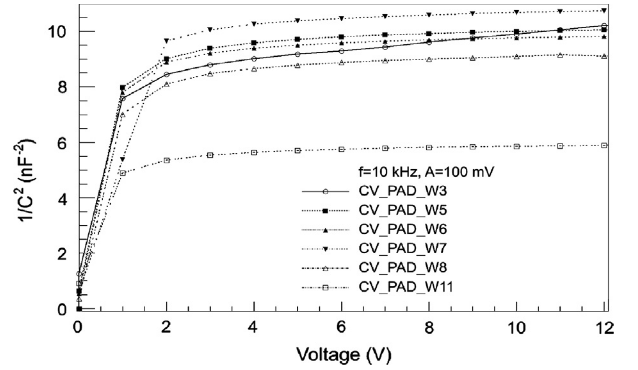

Fig. 5. $1/C^2$ voltage characteristics of 3D pad detectors from every wafer. Wafer 11 (W11) is 230 μm thick while the others are 285 μm thick. The $V_{fd} = 1.5$ V in pads.

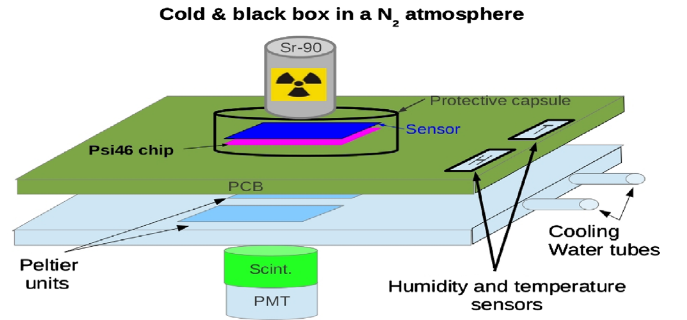

Fig. 6. Test setup for a radioactive source characterization.

chosen to ensure that the sensor is fully depleted:

$$V_{fd} = \frac{Nq}{2\epsilon}\left[r_1^2 Ln\frac{r_2}{r_1} - \frac{1}{2}(r_2^2 - r_1^2)\right]. \quad (1)$$

4. Characterization with a radioactive source

The test setup consists of a ^{90}Sr radioactive source (3.7 MBq) on top of a PCB board carrying the device under test. For triggering, a plastic scintillator read out with a photomultiplier is used. All the components are inside a thermally isolated and light-tight box filled with nitrogen gas. The calibration temperature and humidity are measured by two sensors in contact with the detector PCB board. During the characterization the temperature of the sensors was of −20 °C. Fig. 6 shows the experimental arrangement.

4.1. Unirradiated sensors

In an unirradiated sensor of 285 μm thickness, the electron–hole pairs distribution, that is created when a minimum ionizing particle transverses the silicon bulk, follows a Landau distribution with a mean of 21 400 electron–hole pairs. In our measurement, the collected average value is 21 500 electrons (most probable value is 18 200 electrons), in agreement with the expectations.

4.2. Irradiated sensors

Several sensors were irradiated at Ljubljana TRIGA nuclear reactor (continuous neutron spectrum) and the Karlsruhe proton cyclotron (25 GeV beam); Table 2 summarizes the irradiation fluences.

Out of the total number of irradiated pixel devices, five have been studied: four pixel sensors irradiated up to a fluence of

Table 2
Irradiation fluences and types of particles. Four 3D pixel detectors, two strip detectors and two pads were irradiated for every fluence and particle ID.

Fluences (1 MeV n_{eq}/cm^2)	Particle and facility
$1\times10^{15}, 5\times10^{15}$	Protons in Karlsruhe
$1\times10^{15}, 5\times10^{15}, 1\times10^{16}$	Neutrons in Ljubljana

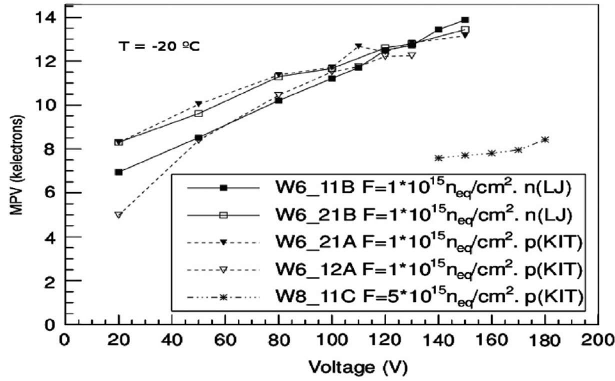

Fig. 7. Most probable value against bias voltages, four samples irradiated up to 1×10^{15} n_{eq}/cm^2 and one up to 5×10^{15} n_{eq}/cm^2.

1×10^{15} n_{eq}/cm^2, two of them with protons and the other two with neutrons and one device irradiated with protons up to 5×10^{15} n_{eq}/cm^2. We did not manage to get to work any PSI46 ROC irradiated to the fluence of 1×10^{16} n_{eq}/cm^2. Fig. 7 shows the most probable value of the collected charge of the studied devices against the bias voltage. The behavior for irradiated detectors up to 1×10^{15} n_{eq}/cm^2 is very homogeneous and similar between different devices independently of the type of radiation type. The comparative study between unirradiated and irradiated sensors shows that the signal is reduced by 30% after irradiation. The device irradiated to a value of 5×10^{15} n_{eq}/cm^2 shows a signal reduction of 55%.

To estimate the full depletion voltage in an irradiated 3D sensor we define an effective relative efficiency E_r as follows:

$$E_r \equiv \frac{Number\ of\ events\ with\ reconstructed\ hits}{Number\ of\ triggered\ events}. \quad (2)$$

We defined the depletion voltage as the biasing voltage for which E_r plateaued. For each device, the absolute value of E_r depends on the bump yield and the relative position between the radioactive source and the triggering scintillator; therefore, to compare the different devices, we normalize each E_r curve to its maximum, as shown in Fig. 8. According to the above definition, the depletion voltage is reached at about 100–120 V for those samples irradiated to a fluence of 1×10^{15} n_{eq}/cm^2. For those samples irradiated to 5×10^{15} n_{eq}/cm^2, the depletion voltage is not well defined. As seen in Fig. 7, the collected charge most probable value is almost flat for any voltage, starting increasing at 180 V, which could indicate avalanche effects, and E_r versus the biasing voltage curve's gradient decreases with the increasing bias voltage. Therefore, we consider the samples irradiated up to 5×10^{15} n_{eq}/cm^2 depleted at a bias voltage of about 180 V.

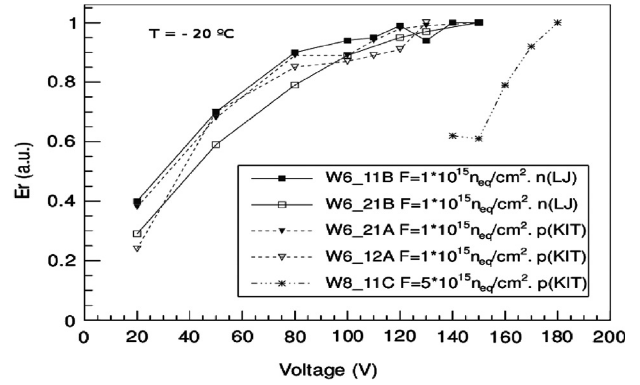

Fig. 8. Relative efficiency, E_r, against bias voltage, showing a $V_{fd}=120$ V for fluences of 1×10^{15} n_{eq}/cm^2 and $V_{fd}=180$ V for fluences of 5×10^{15} n_{eq}/cm^2.

5. Conclusions

We investigated the performance of the 3D double-type double-sided pixel technology up to a fluence of 5×10^{15} n_{eq}/cm^2. At this fluence, a 285 μm thick device delivers a signal of about 8000 electrons for an operating voltage of 180 V; well above the signal threshold setting of the PSI46 readout ASIC. Further investigations are necessary for sensors irradiated beyond 1×10^{16} n_{eq}/cm^2. This study confirms recent results from the ATLAS IBL collaboration [9]. In addition, we successfully demonstrated for the first time the use of a polysilicon resistor grid for the biasing of the sensor prior to its bonding to the readout ASIC.

Acknowledgments

The research underlying this work has been partly supported by the Spanish Ministry of Economy and Competitiveness, Grants FPA2010-22163-C02-01(-02) and FPA2010-22060-C02-01(-02); the European Commission under the FP7 Research Infrastructures project AIDA, Grant agreement no. 262025; and by the GICSERV program “Access to ICTS integrated nano and micro electronics cleanroom” of the Spanish Ministry of Science of Innovation.

Especial thanks to the Karlsruhe and Ljubljana irradiation facility teams, to Silvane Streuli (PSI), Hans Christian Kaetsli (PSI) and Andrey Starodumov (ETH- Zurich) for their scientific, technical support and fruitful discussions.

References

[1] S.I. Parker, C.J. Kenney, J. Segal, Nuclear Instruments & Methods in Physics Research Section A 395 (1997) 328.
[2] D. Penicard, et al., IEEE Transactions on Nuclear Science NS-658 (4, Part 3) (2007) 1435.
[3] M. Kohler, et al., IEEE Transactions on Nuclear Science NS-58 (3) (2007) 1308.
[4] M. Barbero, et al., Nuclear Instruments & Methods in Physics Research Section A 517 (2004) 349.
[5] G. Pellegrini, et al., Nuclear Instruments & Methods in Physics Research Section A 592 (2008) 38.
[6] S.I. Parker, C.J. Kenney, IEEE Transactions on Nuclear Science NS-46 (4) (1999) 1224.
[7] J. LLacer, Nuclear Instruments & Methods in Physics Research 98 (1972) 259.
[8] G. Pellegrini, Technology Development of 3D Detectors for High Energy Physics and Medical Imaging, CERN-THESIS-2006-048, University of Glasgow, 2002.
[9] The ATLAS IBL Collaboration, Prototype ATLAS IBL modules using the FE-I4A front-end readout chip, Journal of Instrumentation 7 (2012) P11010.